- Technical Paper -

SEISMIC PERFORMANCE AND EVALUATION ON A RC RIGID-FRAME ARCH BRIDGE CONSIDERING DAMAGE OF FOUNDATION

Zhongqi SHI[*1], Kenji KOSA[*2], Jiandong ZHANG[*3]and Tatsuo SASAKI[*4]

ABSTRACT

Xiaoyudong Bridge received great damage in Wenchuan Earthquake. As a RC rigid-frame arch bridge, its dynamic behavior was not sufficiently studied. By 2-span dynamic analyses, it is found exposure of pile made P3 more deformable. This caused more severe local failure on Span 4, especially failure of arch leg by axial stress up to 65% f_{ck}. Besides, local failure reduced degree of static indeterminacy, which caused gradual loss of entire stability. Consequently, Span 3 & 4 collapsed into river finally.

Keywords: Wenchuan Earthquake, rigid-frame arch bridge, high axial ratio, failure mechanisms

1. INTRODUCTION

Wenchuan Earthquake occurred in China, at 2:28 p.m. on May 12th, 2008. It had the magnitude of 8.0 measured by CEA and 7.9 by USGS. Report has been published saying 86 bridges suffered extensive damage or entire collapse among 1350 bridges damaged by only seismic effect except geological disasters, and in area with seismic intensity from VII to XI. Authors conducted field damage surveys of Xiaoyudong Bridge, (as elevation drawing shown in Fig. 1) which crossed Baishui River in Xiaoyudong Town on Peng-Bai Road. Based on study on rigid-frame arch bridge, it is a composite structural type of arch bridge and inclined rigid-frame bridge, and a static indeterminate structure with horizontal thrust, which has been abundantly constructed in China since 1980s. By statistical investigation, accumulative total span length of this type of bridge is more than 15,000 km. It indicates that rigid-frame arch bridge is very popular in China.

However, there is still few detailed research on the vibration behavior of this type of bridge. Failure mechanisms of Xiaoyudong Bridge are still not clearly understood. Previously, vibration characteristics of it were studied briefly by 1-span model. Though, failure of pile beneath P3 was not taken into account. Besides, deformation in analysis was not able to reappear the actual damage. Thus, aiming at verifying in-plane vibrate behavior of Xiaoyudong Bridge, and clarifying possible failure mechanisms, nonlinear dynamic analyses by 2-span frame model are conducted. Furthermore, discussion and evaluation about the possible failure mechanisms are conducted.

2. BRIDGE& ANALYTICAL MODELING

2.1 Bridge Structure

Since the design drawings of Xiaoyudong Bridge are not available, dimensions and reinforcement condition have been assumed based on field survey and referred from another RC rigid-frame arch, with almost same characteristics as Xiaoyudong Bridge, for example span length, rise, width-girder ratio and design seismic intensity VII. As being illustrated in Fig. 1, all abutments, piers and spans were numbered from the left bank. According to the results measured by measuring tape, Span 1 has the length of 42.35 m, while Span 2 and Span 3 have the same length of 43.15 m. Thereby, considering the same length of Span 2 and Span 3, and no geographical limitation for piers and abutments, the bridge is considered symmetrical. Due to river went through Span 4, and the girder had collapsed into the water, it was impossible to measure the girder of Span 4. Thus length of Span 4 was assumed as same as Span 1 of 42.35 m, noticing the symmetry of entire bridge.

Arch leg and inclined leg has 21° and 40° slope for each and support the girder in mid-span. Arch frame is formed by arch legs and girder in mid-span. This arch frame, together with two inclined legs and girder at the ends, compose one single rigid-frame. One span

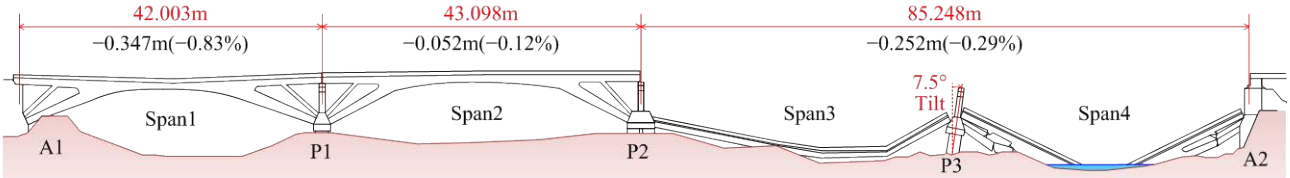

Fig. 1 Elevation view of Xiaoyudong Bridge after the earthquake (view from upstream)

*1 Ph.D. Candidate, Graduate School of Engineering, Kyushu Institute of Technology, JCI Student Member
*2 Ph.D., Prof., Department of Civil Engineering, Kyushu Institute of Technology, JCI Member
*3 Senior Engineer, Jiangsu Transportation Research Institute, China, JCI Member
*4 Manager, Technical Generalization Division, Nippon Engineering Consultants Co., Ltd., JCI Member

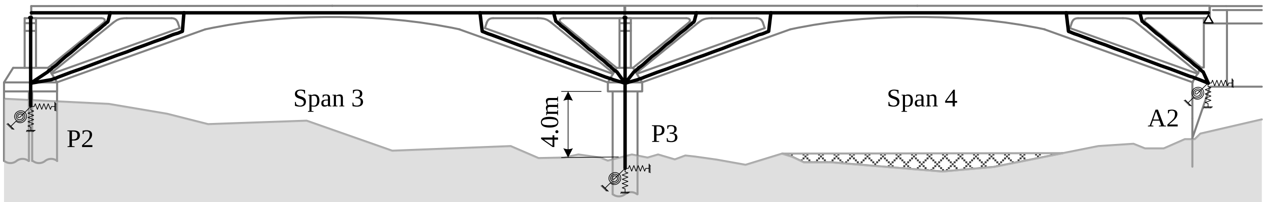

Fig. 2 Analytical model for Span 3 & 4

consists of five rigid-frames connected by beams, arch slab, and extending slab in transverse direction. Then, four spans are supported and connected by piers and abutments. A pier includes a reinforced concrete bending frame with two columns and a beam, upon which two decks are simply supported by rubber bearings. Legs are connected to footing, which is supported by RC piles. For materials, the concrete for Xiaoyudong Bridge is assumed as C30. For the detailed condition of reinforcement, including arrangements, numbers and diameters, on the other hand, it is assumed by utilizing same reinforcement ratio of local members according to Jinzhai No.6 Bridge. Main rebars are assumed as HRB335 (f_y=335 N/mm^2), and the area ratio is 0.72 % and 1.31 % for inclined legs and arch legs, and varies from 1.23 % to 2.27 % for the girder in the mid-span. Besides, stirrups are assumed as HPB235 (f_y=235 N/mm^2) and the volume ratio is 0.19 %, 0.16 % and 0.20 % for inclined legs, arch legs and girder in the mid-span respectively. Similarly, bars for pile beneath P3 are assumed based on the sample as well. Thus, area ratio of main rebar is 0.83 % by HRB335 while volume ratio of stirrups is 0.16 % by HPB235.

2.2 Analytical Modeling and Conditions

As being mentioned for the bridge structure, P2 (the pier between Span 2 and Span 3 with 4 piles beneath it) forms the symmetric axis of entire structure, and Span 3 & 4 collapsed entirely while Span 1 & 2 stood still. Consequently, Span 1 & 2 and Span 3 & 4 can be divided naturally according to not only the structural characteristics but also their actual damage condition. Therefore, 2-span models are made for Span 3 & 4 and Span 1 & 2 separately to verify their possible failure mechanisms and the vibration behavior.

As shown in Fig.2, noticing five arch frames on transversal direction, we select one single arch frame, including slab, to establish 2D model. The pile beneath P3 has been exposed before Wenchuan Earthquake probably due to scouring, which is a special character of Span 3 & 4distinguished from Span 1 & 2 (Fig. 3). After this event, about 7.5º residual tilt, and great damage were observed for P3 and at bottom of pile near the ground surface respectively. Thus, aiming at taking the damage of pile beneath P3 into consideration, tri-linear M-Φ model is set for it, to simulate the exposure of it before the occurring of earthquake. Rigid elements have been set to the following parts: the footing, the beam on the top of the piers and the joints between legs and girder. Tri-linear M-Φ elements calculated based on Japanese specification are used for other parts. Then, M-Φ relationships are calculated considering axial forces when only dead load acts on

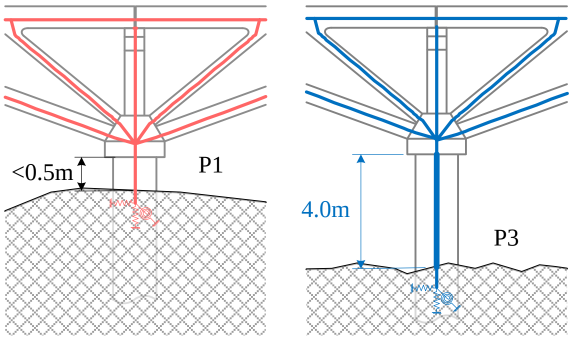

(a) P1 Model for Span 1&2 (b) P3 Model for Span 3&4

Fig. 3 Differences between Span 1&2 VS Span 3&4

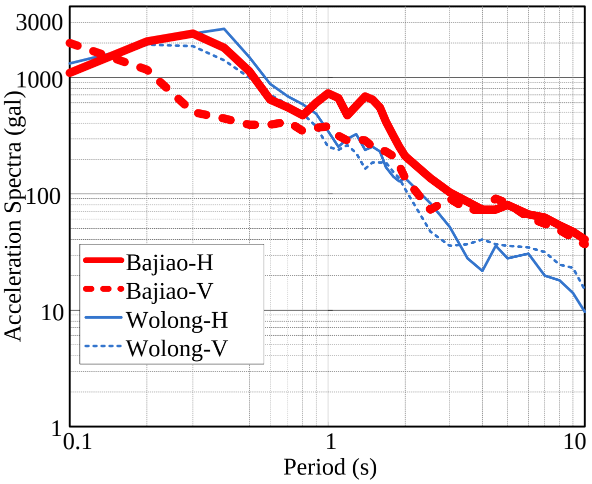

Fig. 4 Acceleration spectra

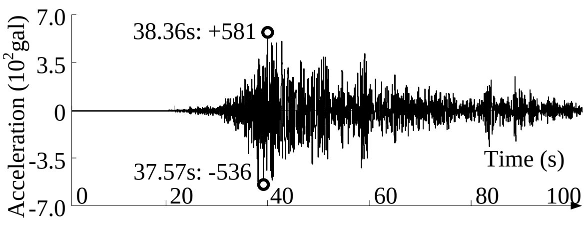

(a) Horizontal Component

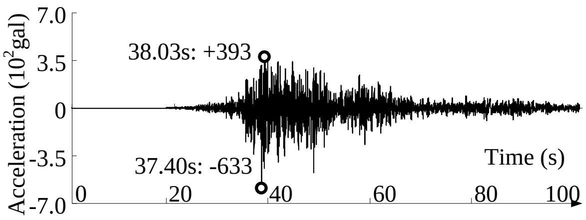

(b) Vertical Component

Fig. 5 Input seismic wave form

the structure. Besides, vertical, horizontal and rotational springs are set under piers and abutments. For springs between girder and pier, a frictional spring which is assumed to be comparatively weak, and a supporting spring are used on pier. On the other hand, frictional and supporting springs are used on top of abutment. Currently, collision spring is not taken into account.

The response acceleration spectra, as shown in Fig. 4, are used to make comparison of the seismic wave by Bajiao Station and Wolong Station in Wenchuan Earthquake. We can see that Bajiao wave can represent the seismic characteristics of Wenchuan Earthquake for its strong horizontal component in low period zone and strong vertical component in general, although it is slightly weaker than Wolong wave. Thanks to the closest distance from Xiaoyudong Bridge of 24 km, Bajiao wave is used in analysis. Both horizontal and vertical components are input (Fig. 5). For the damping, 20% is used for springs at basement, while 2% is used for all other concrete members. Rayleigh damping by eigen-vibration analysis is applied for entire structure. For calculation, Newmark-β (β= 1/4) method is applied in the numerical integration with the time step being 1/1000s.

3. ANALYTICAL RESULTS

Analytical results are going to be introduced generally for girder and legs in Section 3.1, followed by the discussions on the failure of pile beneath P3. Then, evaluations on possible reason of the failure at bottoms of legs are going to be conducted in Section 3.2.

3.1 General Results

Evaluation will be explained for Span 4 comparing with Span 1 as representative. Flexural failure was found to domain the actual damage condition of Xiaoyudong Bridge, while shear failure was only observed for legs on A1 probably due to collision with revetment. No other shear failure was found for the other members. Therefore, the evaluation is mainly determined by the flexural response. Peak plastic ratio is calculated by using Eq. (1) as following:

$$\mu_{max} = \Phi_{max} / \Phi_y \quad (1)$$

where, μ_{max}: peak plastic ratio; Φ_{max}: peak response curvature; Φ_y: yield curvature. Therefore, peak plastic ratio distributions are plotted for Span 4 and Span 1, as shown in Fig. 6 ((a) for girder, (b) for left inclined leg, and (c) for left arch leg as examples). From Fig. 6 (a), we can see that the responses of girder of Span 4 and Span 1 are very similar. For both spans, the greatest peak plastic ratio occurs to the joints between girder and arch legs, and they all reaches beyond the ultimate stage. For Span 4, Point A (joint between girder and arch leg on pier side) reaches at 11.3 (1.10 Φ_u), Point B (joint between girder and arch leg on abutment side) reaches at 12.8 (1.24 Φ_u), while for Span 1, Point A reaches at 11.2 (1.09 Φ_u), Point B reaches at 14.8 (1.44 Φ_u). Although there are slight mathematical differences, they still suggest similar damage condition judging by their peak plastic ratio just beyond the ultimate stage. Furthermore, peak plastic ratio distributions of left legs

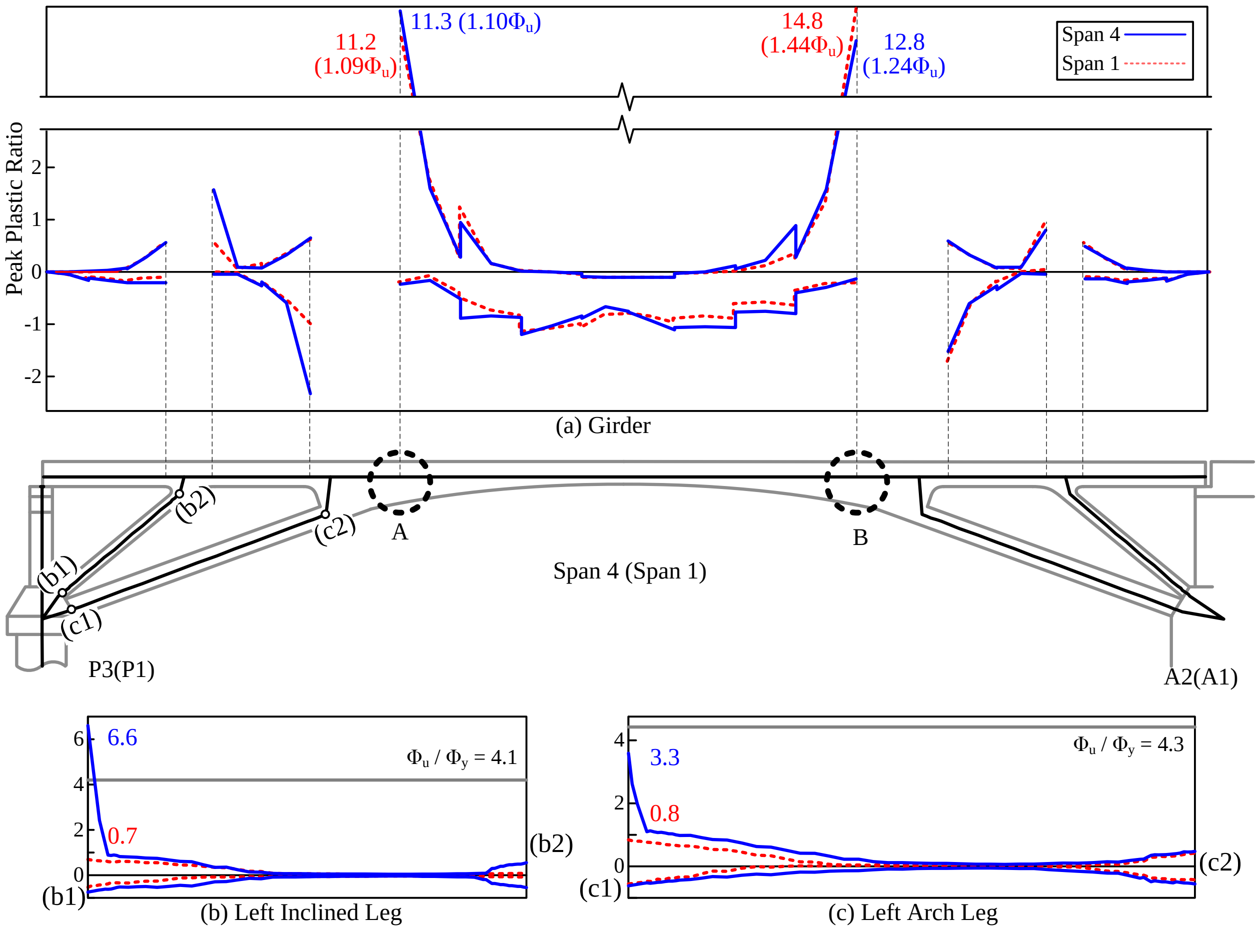

Fig. 6 Comparison of peak plastic ratio distribution between Span 4 and Span 1

are shown in Fig. 6 (b~c) (b1, c1 for bottoms, b2, c2 for tops). As plotted as dot line, no yield can be observed for legs on Span 1 (smaller than 1.0). On the other hand, all bottoms of legs on Span 4 reach over the yield stage. For example, the bottom of left inclined leg on Span 4 (the one connects to footing of P3, Fig. 6 (b)) reaches at 6.6 for maximum. It exceeds the ultimate stage as ultimate curvature is 4.1 times of yield curvature. For the left arch legs on Span 4, bottom of it reaches at 3.3 (77% of ultimate, Fig. 6 (c)). Possible failure of this point is going to be discussed later in Section 3.2.

Besides, for piers, responding deformation of P3 and peak plastic ratio distribution along pile beneath P3 is shown in Fig. 7 (a) and (b) respectively. From Fig. 7 (a), we can see that bending at bottom of pile mainly contributes to the total tilt of P3, and the maximum 6.38cm horizontal displacement towards A2 at 41.36s on top of P3. This can be confirmed in Fig. 7 (b). At bottom of pile beneath P3 (at the ground level where great flexural failure actually occurred to the piles), peak plastic ratio reaches at 2.7 beyond the yield.

Moreover, general displacements (middle point on the girder is taken as representative) are shown in Fig. 8 ((a) for horizontal direction while (b) for vertical direction). It can be observed that Span 1 moves 1.99cm toward A1 for maximum at 41.31s. However, Span 4 moves 3.68cm for most towards A2 at 41.35s, which is about 1.85 times of that for Span 1. For the vertical direction, Span 4 receives great vibration and moves 0.81cm upwards at 41.35s (accompany with the maximum horizontal displacement). Vibration of P3 probably causes these maximum displacements. On the contrary, Span 1 moves limited in the vertical direction.

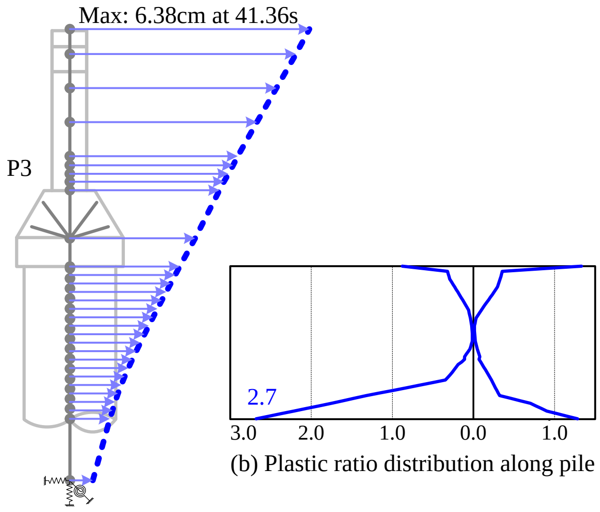

(a) Deformation of P3

(b) Plastic ratio distribution along pile

Fig. 7 Response of pile beneath P3

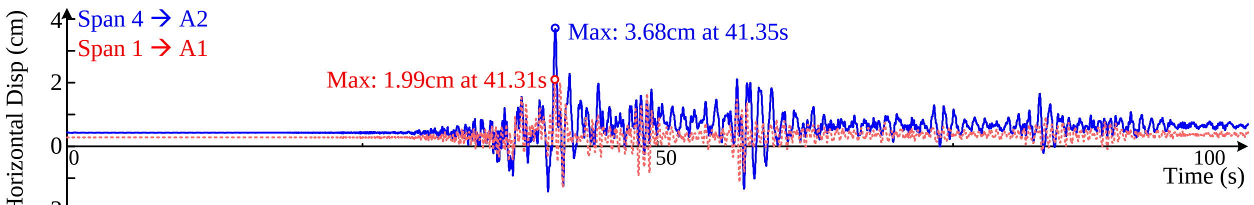

(a) Horizontal Displacement Histories of Girder

(b) Vertical Displacement Histories of Girder

Fig. 8 Comparison on displacement histories of girder

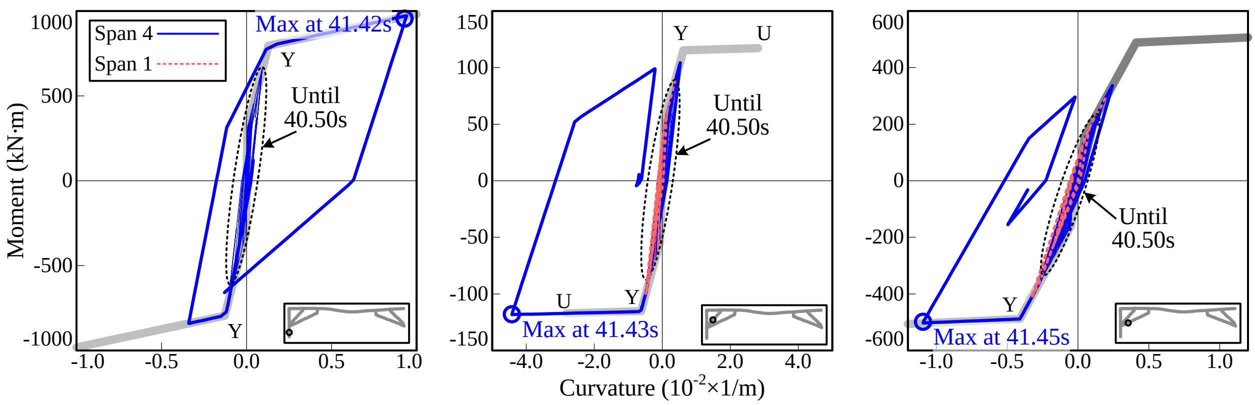

(a) Pile beneath P3

(b) Inclined Legs on P3/P1

(c) Arch Legs on P3/P1

Fig. 9 M-Φ Histories from 0.0s to 42.0s (great plasticity development of members on Span 4)

Table 1 Conditions of specimens in references on ductility of axial loaded RC column

Series	Series A	Series B	Series C	Series D	Series E
References	Reference [1]	Reference [2]		Reference [3]	
Cross Sections unit: mm	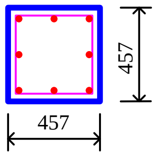	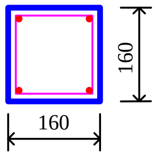		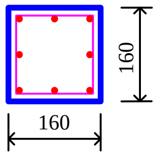	
Longitudinal Bars (area ratio, ρ_s)	9D28.7 f_{yk}=438Mpa (2.48%)	4D10 or 4D13 f_{yk}=364Mpa (0.61% or 1.04%)		9D10 f_{yk}=341Mpa (2.76%)	
Stirrups (volume ratio, ρ_{sti})	D9.5@307 f_{yk}=476Mpa (0.22%)	D6@100 f_{yk}=337Mpa (0.36%)	D6@60 f_{yk}=337Mpa (0.59%)	D4@40 f_{yk}=559Mpa (0.61%)	D4@20 f_{yk}=559Mpa (1.09%)
Number of Specimens	3	12	6	21	14
Axial Ratio	15.1% ~ 60.6%	20.0% ~ 95.0%	40.0% ~ 60.0%	20.0% ~ 100.0%	20.0% ~ 100.0%
Lateral Load	Cyclic Load				

3.2 Failure of Legs

As mentioned in Section 3.1, bottoms of legs on Span 4 received more significant damage comparing with legs on Span 1. The deformation of P3 probably contributes on these damages greatly. M-Φ histories of following three elements are plotted in Fig. 9 for explaining this phenomenon: (a) bottom of pile beneath P3; (b) bottom of inclined legs connecting to P3 on Span 4 VS that connecting to P1 on Span 1; (c) bottom of arch legs connecting to P3 on Span 4 VS that connecting to P1 on Span 1. From these figures, it can be found all elements have had similar level of response before 40.5s, until when no yield occurred to both spans. Then, as deformation of P3 and Span 4 become greater (explained in Fig. 7~8), bottom of pile beneath P3 reaches maximum response at 41.42s, shortly after the max displacement at 41.36s on top of P3. Further, noticeable plasticity is induced at bottoms of both inclined leg and arch leg connecting to P3. They reach maximum at 41.43s and 41.45s soon. Thus, greater damage is triggered with notable residual curvature.

Thus, ultimate stages are able to be confirmed at bottom of inclined legs on Span 4, but still not at bottom of arch legs on Span 4. However, axial load variation is found very significant for arch leg on Span 4. Considering relatively low stirrups ratio in this section, reviews on references on axial-loaded RC columns[1~3] are conducted. Experimental conditions are summarized in Table 1 for 5 series based on different level of stirrups ratio (ρ_{sti}). Their results are plotted in Fig. 10 for displacement ductility (δ_u/δ_y) between axial ratio ($\eta = \sigma_{axial}/f_{ck}$). We can see displacement ductility decreases as axial ratio increases. Especially for specimens with stirrups ratio lower than 0.5% (solid line: approach line for difference series), displacement ductility may drop from about 4.0 (under 20% axial ratio) by 50%, to about 2.0 (under 60% axial ratio). For the analytical result, relationships between max flexural and axial responses of legs on Span 4 are illustrated in Fig. 11. It can be confirmed for Span 4, both inclined legs reach great peak plastic ratio, exceeding ultimate

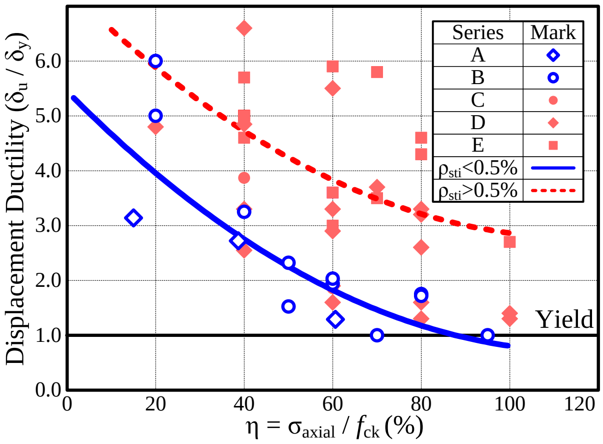

Fig. 10 Ductility by axial load and stirrups ratio

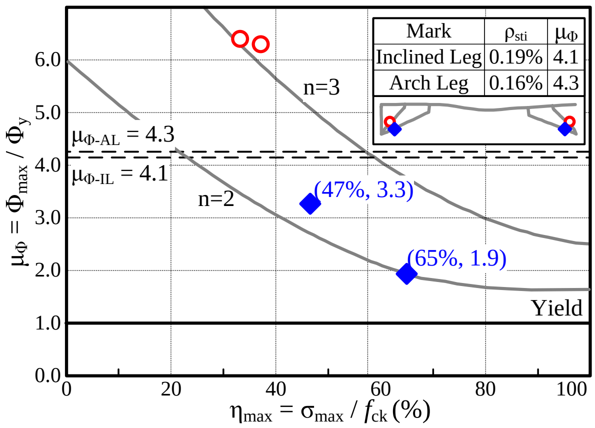

Fig. 11 Max flexural & axial response of legs

stage (6.6 or 6.4> 4.1), even ignoring the axial ratio increase. But arch legs on Span 4 reaches at (47%, 3.3) and (65%, 1.9) respectively, which does not exceed ultimate stage of 4.3. Besides, experimental tests were conducted for axial-loaded columns[4] (in term of δ). By integrating Φ along height to correspond to δ on top of column in experimental tests, Φ at bottom cross sections was calculated. Thus, experiential relation between δ and Φ after yield stage is given by Eq.(2)

based on these experiments and calculations:

$$\Phi = n \times \delta \ (\Phi > \Phi_y,\ n = 2\sim3) \quad (2)$$

Therefore, the solid line (relation between μ_δ and η when ρ_{sti}<0.50%) in Fig. 10 can be redrawn in Fig. 11 (relation between μ_Φ and η). For example when n=2, curve is got by assuming $\mu_\Phi = 2 \times \mu_\delta$, for same η. We can see that although maximum responses of arch legs do not exceed n=3, they locates on the upper zone than line of n=2. Considering there are even less stirrups in arch leg (ρ_{sti}=0.16%), they have notable possibility to reach ultimate stage and to suffer noticeable damage.

Besides, P-δ histories in experiments of Series A are shown in Fig. 12. It can be confirmed that under higher axial ratio, it is hard for RC column with low ρ_{sti} to hold the load in a particular level after ultimate stage (A2 specimen lost its capacity almost immediately after ultimate). Thus, they may lose capacity in all axial, lateral and flexural directions due to high axial ratio and low stirrups ratio. Considering even lower ρ_{sti} for Xiaoyudong Bridge (0.19%, 0.16% and 0.20% for inclined legs, arch legs and girder), it is suitable to ignore any capacity after ultimate of local member.

4. POSSIBLE FAILURE MECHANISMS

For possible failure mechanisms, simplified 1/2 span mechanical model will be used for explanation, using Degree of Static Indeterminate (DSI in following). As a rigid-frame structure, we can get DSI of this 1/2 span model being 6 at initial stage. Explained in Fig. 12, capacity in all three directions is suitable to be ignored considering high axial ratio and low stirrups ratio, which indicates that DSI will decrease by 3 with one ultimate stage of local member. As shown in Fig. 13 (a), by ultimate stages at Point a and b, structural DSI will increase from 6 to 0, which stands for that structure becomes static determinate and any further local failure and loss of DSI will result in entire failure of structure. Explained in Section 3.2, extremely high axial ratio may probably induce capacity loss of arch legs as well. Therefore, this failure at Point c will destroy the structure and cause collapse as shown in Fig. 13 (b). From another point of view, ultimate stages at Point a and b (in Fig. 13 (a)) will isolate arch leg from being connected with girder and inclined leg, and make arch leg a cantilever-like system. Then, due to possible ultimate stage of Point c, clock-wise rotation (Fig. 13 (b)) will occur on this cantilever-like system. As a consequence, Span 4 probably collapsed entirely. On the other hand, without any ultimate at bottom of legs, it is difficult for Span 1 to collapse entirely.

5. CONCLUSIONS

Based on dynamic analyses and comparison by 2-span model, and the reasoning of possible failure mechanisms, following conclusions have been drawn:

(1) Based on dynamic analyses, girder joints with arch leg might suffer ultimate stage for all spans. However, exposure of pile beneath P3 induced notable vibration of P3 and caused more severe failure at bottoms of legs on Span 4. Both inclined legs on Span 4 suffered ultimate stage due to this reason. Furthermore, due to high axial ratio and low stirrups ratio, ultimate stage might also occur to arch legs on Span 4.

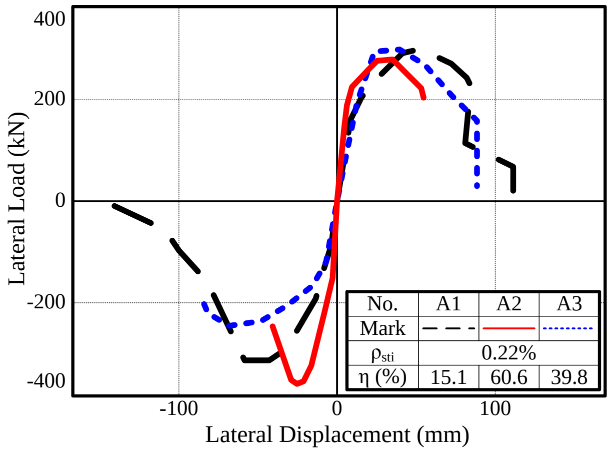

Fig. 12 Capacity loss after ultimate stage

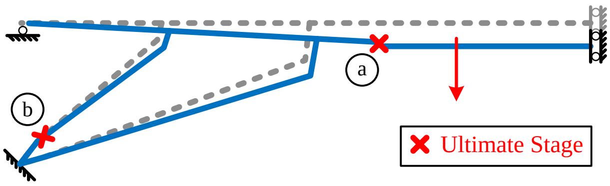

(a) Ultimate Stages of Point a and b

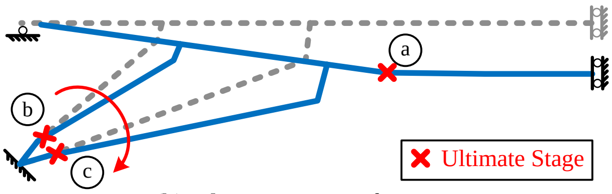

(b) Ultimate Stage of Point c

Fig. 13 Possible failure mechanisms for Span 4

(2) For possible failure mechanisms, stability of Span 4 was weakened by local damages gradually. It might collapse due to ultimate stage at 3 points: girder joint with arch leg, bottom of inclined leg and bottom of arch leg. On the other hand, Span 1 probably survived from entire collapse without any obvious failure at bottom of legs.

REFERENCES

[1] Sezen, H. et al., “Seismic Tests of Concrete Columns with Light Transverse Reinforcement”, ACI Structural Jr., Vol. 103, No. 6, 2006, pp. 842-849

[2] Zhou, X. et al., “Strength and Ductility of Reinforced Concrete Column under High Axial Load”, Proc. of JCI, Vol. 8, 1986, pp. 505-508

[3] Zhou, X. et al., “Behavior of Reinforced Concrete Short Column under High Axial Load”, Proc. of JCI, Vol. 9, 1987, pp. 139-144

[4] Kosa, K. et al., “Evaluation of Earthquake -Damaged RC Piers by the Ultimate Bearing Capacity Procedures”, Jr. of JSCE, No. 592/V-39, 1998, pp. 73-82